Available online at www.sciencedirect.com
ScienceDirect
Procedia Engineering 14 (2011) 2593–2600
Procedia Engineering
www.elsevier.com/locate/procedia

The Twelfth East Asia-Pacific Conference on Structural Engineering and Construction

Field Measurement and Bayesian Modal Identification of a Primary-Secondary Structure

S. K. AU , F. L. ZHANG*

Department of Building and Construction, City University of Hong Kong, China

Abstract

The Mong-Man-Wai Building (MMW) is a seven-storied reinforced concrete building situated on the campus of the City University of Hong Kong. On its roof a two-storied steel frame has been recently constructed to host a new wind tunnel laboratory, forming a primary-secondary structure. This paper presents field instrumentation and modal identification of the structural system. A number of setups were carried out to cover all locations of interest using a limited number of triaxial sensors. Ambient vibration measurements were obtained and modal identification was performed using a Bayesian FFT Approach. The approach views modal identification as an inference problem where probability is used as a measure for the relative plausibility of outcomes given a model of the response and measured data. The modal identification results reveal a number of interesting features about the building and the roof frame. Five modes are presented in this paper, exhibiting the dynamics of the primary and secondary structure as well as their coupling.

Selection

Keywords: MMW building, ambient test, Bayesian FFT Approach, modal identification

1. Introduction

The response of a structure subjected to dynamic loads is characterized by its modal properties, including the natural frequencies, damping ratios and mode shapes. Knowing the natural frequencies of a structure can help assess potential resonance problems and design necessary measures to alleviate them. The damping ratio is also an important attribute affecting the energy dissipation of the structure and hence

* Corresponding author
Email: fzhang7@student.cityu.edu.hk
* Presenter
Email: fzhang7@student.cityu.edu.hk

doi:10.1016/j.proeng.2011.07.326

the vibration amplitude. Much research has been performed (Hart 1996; Satake et al. 2003). When designing a structure, the damping ratio is usually assumed to be constant. However, in reality there is a large variation in the damping ratio. Knowing the actual damping ratio can help better assess the dynamic response. It can also provide experience to structure designers. The mode shape of a structure reflects the distribution of stiffness and mass as well as boundary conditions. The change in mode shape across major loading events may also be used for damage detection or, more generally, structure health monitoring (Sohn et al. 2003).

Compared with force vibration test and free vibration test, ambient vibration test is more economical for full-scale buildings (e.g., Beck et al. 1997; Brownjohn 2003). In this test, vibration data is acquired when the structure is under unknown but statistically random working load. The signal-to-noise ratio cannot be directly controlled, and so if the noise level is too high, it will be difficult to identify the modal properties. The success of an ambient vibration test hinges on the achievable signal-to-noise ratio and whether interference from unknown colored excitations in the interested frequency band is significant. This is an area that can only be explored with practical implementation and full-scale field data.

This paper presents work on modal identification using ambient vibration data obtained from the Mong Man-Wai building, at the City University of Hong Kong. A two-storied steel frame has been constructed on the roof of the building, making it a primary-secondary structure. The building is connected through expansion joints to its neighboring structures, which also influence the mode shapes. Modal identification is performed based on a Bayesian FFT Approach, whose theory will be briefly outlined. Simplifications are made to speed up computation, taking into account typical data configuration applicable in practice.

2. Description of the MMW Building

The Mong Man-Wai (MMW) building is situated on the campus of the City University of Hong Kong. It is an office building of mainly concrete construction. Figure 1 shows the front view of the building. It has seven floors. A two-storied steel frame has been constructed recently on the roof to host a new wind tunnel laboratory. Figure 2 shows a schematic diagram of the structure. The roof frame and the MMW building can be considered as a primary-secondary structure. The MMW building is supported by bulky columns. Its lateral system is assisted by shear walls near the lift shafts on the left and right side of the building in Figure 2. The roof frame is supported directly on the main columns of the MMW building. The MMW building is not an independent structure. At the left corner and the back corner, it is connected to two different buildings.

3. Instrumentation

Figure 2 shows the locations where measurements were obtained. At each typical floor only measurements at the left and right staircase were obtained. As shown in Figure 2, it was targeted to obtain triaxial measurement at 36 locations, giving a total of 108 degrees of freedom (DOFs). The first 54 DOFs for Location 2101 to Location 2212 are on the roof of the building. Three setups were designed to measure these locations in order to observe the vibration of the roof frame. The next 36 DOFs for Location 1201 to 1702 are at the staircases near the shear walls of the building. Note that the orientations of these two sets of DOFs differ by an angle of 45 degrees. The orientations of sensors in the first 18 locations were along the long direction of the roof frame, as it was easier to perform sensor alignment. In order to examine rigid floor assumption of the MMW building that connected the two shear walls, 18 DOFs for Location 1703 to 1708 forming a line on the roof of the building were also measured. The orientations in these locations are same with those in the locations from 1201 to 1702.

Figure 1: Front view of MMW Building

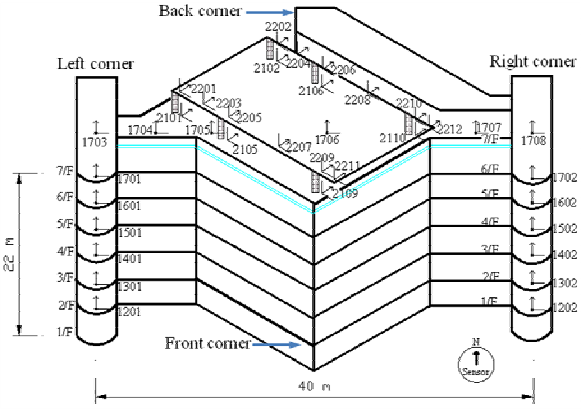

Figure 2: Schematic diagram of MMW Building

Table 1: Setup plan (location numbers)

Channel/ Setups	1, 2, 3	4, 5, 6	7, 8, 9	10, 11, 12	13, 14, 15	16, 17, 18	19, 20, 21	22, 23, 24
1	2109	2209	2201	2202	2205	2206	2209	2210
2	2109	2209	2203	2204	2207	2208	2211	2212
3	2109	2209	2101	2102	2105	2106	2109	2110
4	2109	2209	1708	1707	1706	1705	1704	1703
5	2109	2209	1701	1601	1501	1401	1301	1201
6	2109	2209	1702	1602	1502	1402	1302	1202

The number of the sensors is not enough to measure 108 DOFs at a time and only 24 channels at 8 locations can be measured at each setup. Obtaining mode shape from separate setups and assembling modes is thus inevitable. Reference channels are necessary for assembling modes from different setups. To be on the safe side reference channels were set on both the main building and the first floor of the roof frame. The six DOFs for Location 2109 and 2209 served as reference DOFs. Based on this, six setups in Table 1 were designed to cover all the DOFs of interest.

4. Bayesian FFT Approach

The theory of Bayesian Fast Fourier Transform (FFT) Approach is briefly described here. The reader is referred to Yuen and Katafygiotis (2003) for details. The basic idea is that, for a structure under broad-banded excitation, the real part and the imaginary part of the FFT of the structural response follows a multi-dimensional Gaussian distribution. By maximizing the posterior PDF of modal parameters given the FFT data, or equivalently minimizing the log-likelihood function, the most probable modal properties can be determined.

The measured acceleration data is assumed to consist of the structural ambient vibration signal and prediction error:

$$\underline{\ddot{y}}(j) = \underline{\ddot{x}}(j) + \underline{\varepsilon}(j) \tag{1}$$

where $\underline{\ddot{x}}(j) \in R^n$ and $\underline{\varepsilon}(j) \in R^n$ (j=1,2,…,N) are the acceleration response of the structure and prediction error, respectively; N is the number of sampling points; n is the number of measured DOFs. The FFT of $\underline{\ddot{y}}(j)$ is defined as

$$F_{\underline{\ddot{y}}}(\omega_k) = \sqrt{\frac{2\Delta t}{N}} \sum_{j=0}^{N-1} \underline{\ddot{y}}(j) e^{-\mathbf{i}\omega_k j\Delta t} \tag{2}$$

where $\omega_k = k\Delta\omega, k = 0,1,...N_1 - 1$ with $N_1 = INT[(N+1)/2]$, $\Delta\omega = 2\pi/T$; $INT[.]$ denotes the integer part of its argument; T is the data duration; $\Delta t = 1/f_s$; f_s is the sampling frequency.

Let $\underline{\theta}$ denote the modal parameters to be identified and $Z(\omega_k) = [\mathrm{Re}\, F_{\underline{\ddot{y}}}(\omega_k)^T, \mathrm{Im}\, F_{\underline{\ddot{y}}}(\omega_k)^T]^T$ be an augmented vector of the real part and imaginary part of the model FFT. Using Bayes' Theorem, the posterior PDF of $\underline{\theta}$ given the data is given by:

$$p(\underline{\theta} \mid \tilde{Z}) = cp(\underline{\theta})\, p(\tilde{Z} \mid \underline{\theta}) \tag{3}$$

where c is a normalizing constant; $p(\underline{\theta})$ is the prior PDF that reflects the plausibility of $\underline{\theta}$ in the absence of data; $\tilde{Z} = [\tilde{Z}(\omega_{k_1}),..., \tilde{Z}(\omega_{k_2})]$ is a collection of the FFT data confined to a selected frequency band from ω_{k_1} to ω_{k_2}. The 'most probable value' (MPV) of modal parameters $\underline{\theta}$ is the one that maximizes $p(\underline{\theta} \mid \tilde{Z})$. Numerically it is more convenient to work with the log-likelihood function:

$$L(\underline{\theta}) = -\ln p(\underline{\theta} \mid \tilde{Z}) \tag{4}$$

Minimizing $L(\underline{\theta})$ is equivalent to maximizing $p(\underline{\theta} \mid \tilde{Z})$. For large N and small Δt. It can be shown that the FFT at different frequencies are asymptotically independent and they follow a Gaussian distribution. The likelihood function $p(\tilde{Z} \mid \underline{\theta})$ is then given by:

$$p(\tilde{Z} \mid \underline{\theta}) = \prod_{k=k_1}^{k_2} (2\pi)^{-n} |C_k|^{-\frac{1}{2}} \times \exp[-\frac{1}{2} \tilde{Z}^T(\omega_k)(C_k)^{-1} \tilde{Z}(\omega_k)] \tag{5}$$

where $|\cdot|$ denotes the determinant; C_k is the covariance of the augmented FFT vector:

$$C_k = E[Z(\omega_k) Z(\omega_k)^T] = \begin{bmatrix} E[\mathrm{Re}\, F_{\ddot{x}}(\omega_k)\, \mathrm{Re}\, F_{\ddot{x}}^T(\omega_k)] & E[\mathrm{Re}\, F_{\ddot{x}}(\omega_k)\, \mathrm{Im}\, F_{\ddot{x}}^T(\omega_k)] \\ E[\mathrm{Re}\, F_{\ddot{x}}(\omega_k)\, \mathrm{Im}\, F_{\ddot{x}}^T(\omega_k)] & E[\mathrm{Im}\, F_{\ddot{x}}(\omega_k)\, \mathrm{Im}\, F_{\ddot{x}}^T(\omega_k)] \end{bmatrix} + \frac{1}{2}\mathbf{S}_{\varepsilon} \tag{6}$$

where $\mathrm{E}[.]$ denotes the expectation. The covariance matrix C_k is related to the set of modal parameters $\underline{\theta}$ to be identified, which includes three groups of parameters. The first group is $\omega_j, \zeta_j, \varphi_j, j = 1,...m$, where ω_j and ζ_j represent the natural frequency and damping ratio of the j-th mode, respectively; $\varphi_j \in R^n$ is the j-th mode shape vector; m is the number of modes. The second group is $\mathbf{S}_{\mathbf{f}} \in R^{m \times m}$, the power spectral density matrix of modal forces. The third group is $\mathbf{S}_{\varepsilon} \in R^{2n \times 2n}$, the power spectral density matrix of prediction error and whose elements except the diagonal ones are all zeros. For modal identification it is necessary to express C_k analytically in terms of $\underline{\theta}$. The reader is referred to Yuen & Katafygiotis (2003) for the original derivation. A simplified derivation is presented here, taking advantage of large N and small Δt applicable in practical situations. For given $r, s = 1, 2, ...n$, it can be shown using trigonometric relations that:

$$F_{\ddot{x}_r}(\omega_k) F_{\ddot{x}_s}^*(\omega_k) = \left(\sqrt{\frac{2\Delta t}{N}}\right)^2 \sum_{p,q=0}^{N-1} \ddot{x}_r(p) \ddot{x}_s(q) [\cos((p-q)\omega_k \Delta t) - \mathbf{i} \sin((p-q)\omega_k \Delta t)] \tag{7}$$

$$F_{\ddot{x}_r}(\omega_k)F_{\ddot{x}_s}(\omega_k)=\left(\sqrt{\frac{2\Delta t}{N}}\right)^2\sum_{p,q=0}^{N-1}\ddot{x}_r(p)\ddot{x}_s(q)[\cos((p+q)\omega_k\Delta t)-\mathbf{i}\sin((p+q)\omega_k\Delta t)] \tag{8}$$

where '*' denotes the Hermitian operation (conjugate transpose) of the matrix. Using (7) and (8),

$$\begin{aligned}&\mathrm{Re}\,F_{\ddot{x}_r}(\omega_k)\,\mathrm{Re}\,F_{\ddot{x}_s}(\omega_k)\\&=\left(\sqrt{\frac{2\Delta t}{N}}\right)^2\sum_{p,q=0}^{N-1}\ddot{x}_r(p)\ddot{x}_s(q)\frac{1}{2}[\cos((p+q)\omega_k\Delta t)+\cos((p-q)\omega_k\Delta t)]\\&=\frac{1}{2}\mathrm{Re}[F_{\ddot{x}_r}(\omega_k)F_{\ddot{x}_s}{}^*(\omega_k)]+\frac{1}{2}\mathrm{Re}[F_{\ddot{x}_r}(\omega_k)F_{\ddot{x}_s}(\omega_k)]\end{aligned} \tag{9}$$

$$\mathrm{Im}\,F_{\ddot{x}_r}(\omega_k)\,\mathrm{Im}\,F_{\ddot{x}_s}(\omega_k)=\frac{1}{2}\mathrm{Re}[F_{\ddot{x}_r}(\omega_k)F_{\ddot{x}_s}{}^*(\omega_k)]-\frac{1}{2}\mathrm{Re}[F_{\ddot{x}_r}(\omega_k)F_{\ddot{x}_s}(\omega_k)] \tag{10}$$

$$\mathrm{Re}\,F_{\ddot{x}_r}(\omega_k)\,\mathrm{Im}\,F_{\ddot{x}_s}(\omega_k)=-\frac{1}{2}\mathrm{Im}[F_{\ddot{x}_r}(\omega_k)F_{\ddot{x}_s}{}^*(\omega_k)]+\frac{1}{2}\mathrm{Im}[F_{\ddot{x}_r}(\omega_k)F_{\ddot{x}_s}(\omega_k)] \tag{11}$$

$$\mathrm{Im}\,F_{\ddot{x}_r}(\omega_k)\,\mathrm{Re}\,F_{\ddot{x}_s}(\omega_k)=\frac{1}{2}\mathrm{Im}[F_{\ddot{x}_r}(\omega_k)F_{\ddot{x}_s}{}^*(\omega_k)]+\frac{1}{2}\mathrm{Im}[F_{\ddot{x}_r}(\omega_k)F_{\ddot{x}_s}(\omega_k)] \tag{12}$$

where $\mathrm{Re}[.]$ and $\mathrm{Im}[.]$ denote the real part and imaginary part of its argument, respectively.
Expressing the response as a superposition of contributing modes in the spectral domain, for large N and small Δt, it can be shown that:

$$E[F_{\ddot{x}}(\omega)F_{\ddot{x}}^*(\omega)]=\sum_{j=1}^{m}\sum_{k=1}^{m}\varphi_j\varphi_k{}^{\mathrm{T}}S_{f_{jk}}/[(1-(\frac{\omega_j}{\omega})^2)-2\mathbf{i}\zeta_j\frac{\omega_k}{\omega}]/[(1-(\frac{\omega_k}{\omega})^2)+2\mathbf{i}\zeta_k\frac{\omega_k}{\omega}] \tag{13}$$

where $S_{f_{jk}}=E[F_{f_j}(\omega)F_{f_k}{}^*(\omega)]$ is the (j,k) element of $\mathbf{S_f}$. This means that:

$$E[F_{\ddot{x}}(\omega)F_{\ddot{x}}^*(\omega)]=\mathbf{\Phi H \Phi}^T \tag{14}$$

where the (j,k) element H_{jk} in matrix $\mathbf{H}$ can be written as:

$$H_{jk}=S_{f_{jk}}/[(1-(\frac{\omega_j}{\omega})^2)-2\mathbf{i}\zeta_j\frac{\omega_j}{\omega}]/[(1-(\frac{\omega_k}{\omega})^2)+2\mathbf{i}\zeta_k\frac{\omega_k}{\omega}] \tag{15}$$

Similarly, it can be proven that:

$$E[F_{\ddot{x}}(\omega)F_{\ddot{x}}^T(\omega)]=\mathbf{\Phi H}'\mathbf{\Phi}^T \tag{16}$$

where the (j,k) element H'_{jk} in matrix $\mathbf{H}'$ can be written as:

$$H'_{jk}=E[F_{f_j}(\omega)F_{f_k}{}^T(\omega)]/[(1-(\frac{\omega_j}{\omega})^2)-2\mathbf{i}\zeta_j\frac{\omega_j}{\omega}]/[(1-(\frac{\omega_k}{\omega})^2)-2\mathbf{i}\zeta_k\frac{\omega_k}{\omega}] \tag{17}$$

Substituting (9) to (12) into (6), it can be obtained that:

$$C_k=\frac{1}{2}\begin{bmatrix}\mathbf{\Phi} & \\ & \mathbf{\Phi}\end{bmatrix}\begin{bmatrix}\mathrm{Re}\mathbf{H} & -\mathrm{Im}\mathbf{H}\\ \mathrm{Im}\mathbf{H} & \mathrm{Re}\mathbf{H}\end{bmatrix}\begin{bmatrix}\mathbf{\Phi}^T & \\ & \mathbf{\Phi}^T\end{bmatrix}+\frac{1}{2}\begin{bmatrix}\mathbf{\Phi} & \\ & \mathbf{\Phi}\end{bmatrix}\begin{bmatrix}\mathrm{Re}\mathbf{H}' & \mathrm{Im}\mathbf{H}'\\ \mathrm{Im}\mathbf{H}' & -\mathrm{Re}\mathbf{H}'\end{bmatrix}\begin{bmatrix}\mathbf{\Phi}^T & \\ & \mathbf{\Phi}^T\end{bmatrix}+\frac{1}{2}\mathbf{S}_{\boldsymbol{\varepsilon}} \tag{18}$$

where $\boldsymbol{\Phi} = [\varphi_1, \varphi_2, ..., \varphi_m]$ is the $n-by-m$ mode shape matrix. It can be shown that for large N and small Δt, the term associated with $H^{'}_{f_{jk}}$ in the likelihood function is dominated by that associated with $H_{f_{jk}}$. Thus, asymptotically,

$$C_k = \frac{1}{2}\begin{bmatrix} \boldsymbol{\Phi} & \\ & \boldsymbol{\Phi} \end{bmatrix}\begin{bmatrix} \mathrm{Re}\mathbf{H} & -\mathrm{Im}\mathbf{H} \\ \mathrm{Im}\mathbf{H} & \mathrm{Re}\mathbf{H} \end{bmatrix}\begin{bmatrix} \boldsymbol{\Phi}^T & \\ & \boldsymbol{\Phi}^T \end{bmatrix} + \frac{1}{2}\mathbf{S}_\varepsilon \tag{19}$$

5. Modal Identification Results

Using the Bayesian FFT Approach, six sets of natural frequencies, damping ratios and mode shapes have been obtained. A least-square approach (Au 2011) is used to assemble the mode shapes obtained in the six setups. Only the most probable values of modal parameters are presented here in detail, although the Bayesian FFT Approach also yields their posterior uncertainties, which is especially important for ambient vibration tests.

Figure 3 shows the mode shape of the lowest mode with a natural frequency of 2.16Hz and a damping ratio of 1.07%. Due to the two shear walls on the left and right side, the weak and strong direction of the building are oriented parallel to the X-axis and Y-axis, respectively. This is the whole building translational mode in its weak direction as the roof frame moves with the MMW building. It can be seen that there is a rotation about a center near the far top of the figure. This is perhaps because of connections at the back corner with another building. The MMW building tends to rotate about the connection in this mode. Figure 4 shows the mode shape of the mode with a natural frequency of 2.44Hz and a damping ratio of 1.56%.This mode is quite different from the previous one. The whole building translates along the long direction of roof frame. This mode can be considered to result from coupling of dynamics between the main building and the roof frame. Figure 5 shows the mode shape of the mode with a natural frequency of 4.15Hz and a damping ratio of 1.14%. This is a torsional mode of the whole building. The movement of the back-left side of the roof frame is larger than that of the front-right side. Figure 6 shows the mode shape of the mode with a natural frequency of 6.03Hz and a damping ratio of 1.13%. The thin line and the broad line in the left sub-figure represent the raw shape and the moved shape of the structure, respectively. The roof slab of the building vibrates vertically, while the two shear walls of the structure remain relatively stationary. The roof frame vibrates with the slab. The movement in the horizontal direction is quite small compared to that in the vertical direction. Figure 7 shows the mode shape of the mode with a natural frequency of 7.29Hz and a damping ratio of 1.37%. This is dominantly the torsional mode of the roof frame, while the main building remains relatively stationary. By calculating the uncertainties of the identified modal parameters using finite difference, it is found that the coefficient of variation (c.o.v) of the natural frequencies are all below 1%, while the c.o.v of the damping ratios are in the order of a few tens percent, much higher than the counterparts of the natural frequencies.

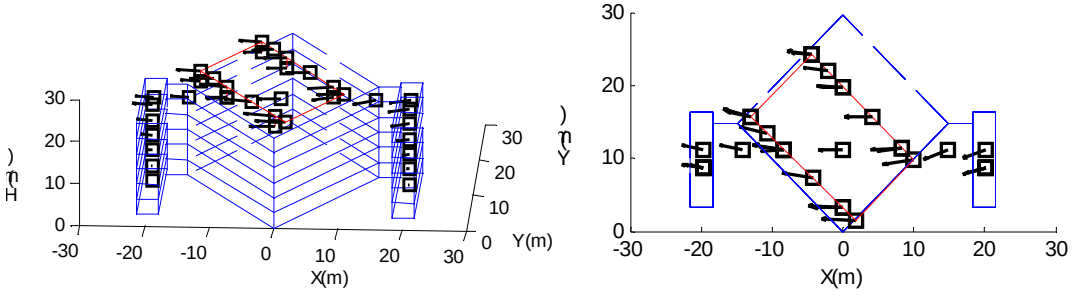

Figure 3: Mode shape with f=2.16 Hz, damping ratio=1.07% (isometric view and plan view)

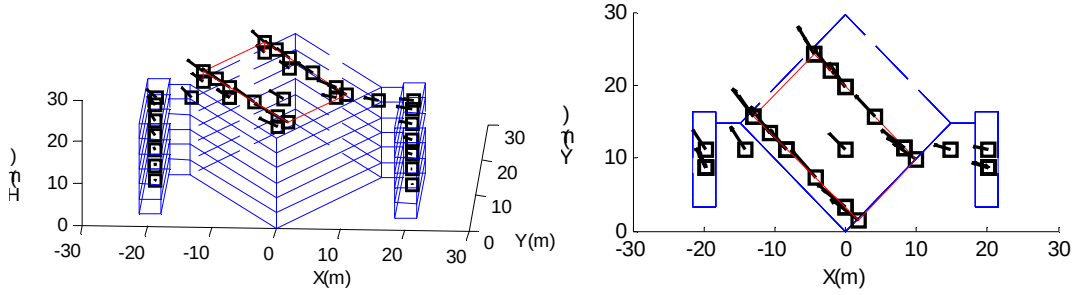

Figure 4: Mode shape with f=2.44 Hz, damping ratio=1.56% (isometric view and plan view)

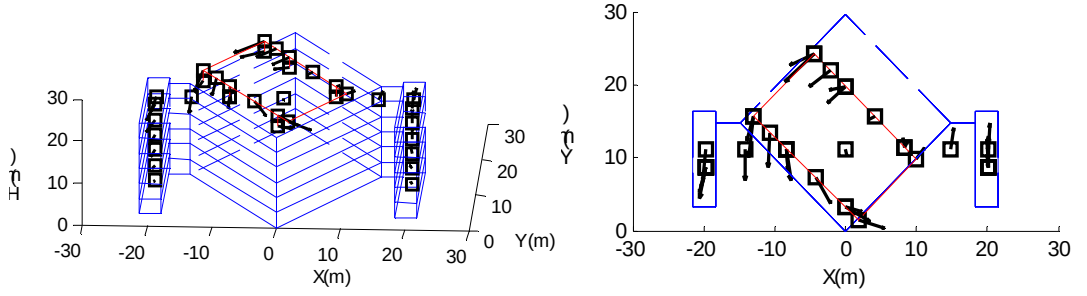

Figure 5: Mode shape with f=4.15 Hz, damping ratio=1.14% (isometric view and plan view)

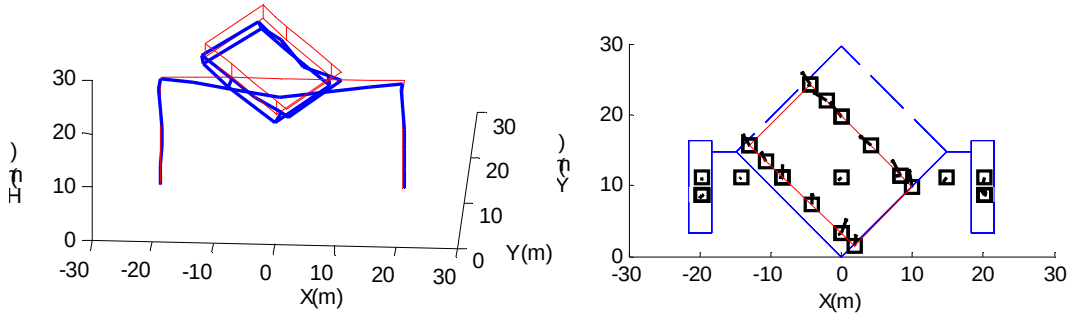

Figure 6: Mode shape with f=6.03 Hz, damping ratio=1.13% (isometric view and plan view)

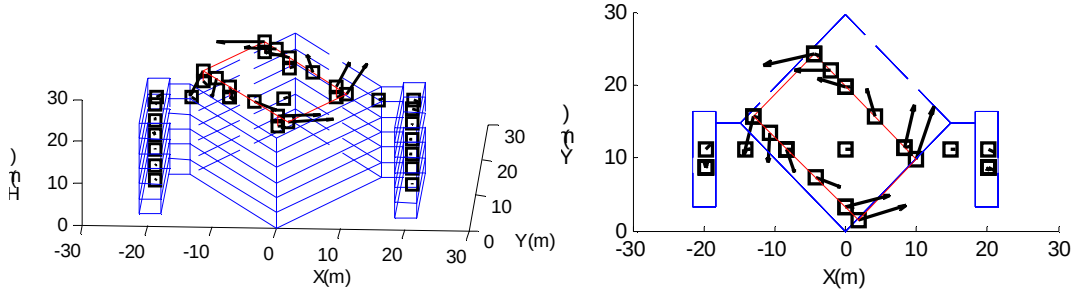

Figure 7: Mode shape with f=7.29 Hz, damping ratio=1.37% (isometric view and plan view)

6. Conclusion

This paper has presented work on ambient vibration test of a full-scale primary-secondary structure and modal identification using the Bayesian FFT Approach. The first four modes presented are attributed to dynamics of the primary structure. The last mode is dominantly due to the roof frame. The expansion joints between MMW building and its neighbouring buildings are found to influence the mode shapes. The damping ratios of the identified modes are all around 1% to 2%. In the modal identification process, there are a total of 28 parameters needed to be numerically optimized in every setup, which is very time consuming. A typical setup requires 3 or 4 hours for modal identification. Research is under way to speed up computations.

Acknowledgments

This paper is funded by the Hong Kong Research Grant Council through General Research Fund (Project No.CityU 110109; 9041484). The financial support is gratefully acknowledged. Ms Yan Chun Ni, graduate student at CityU, participated in the field tests. The authors would like to thank Mr Sy, technical staff at the Wind Tunnel Laboratory, for providing logistics support for the tests.

References

[1] Au SK (2011). Assembling mode shapes by least squares. Mechanical Systems and Signal Processing. To appear.

[2] Beck JL, Vanik MW, Polidori DC, and May BS (1997). Ambient vibration surveys of a steel frame building in a healthy and damaged state. Tech. Rep. EERL 97-03, California Institute of Technology, Earthquake Engineering Research Laboratory, Pasadena, California.

[3] Brownjohn JMW (2003). Ambient vibration studies for system identification of tall buildings. Earthquake Engineering and Structural Dynamics, 32, pp. 71-95.

[4] Hart GC. (1996). Random damping in buildings. Journal of Wind Engineering and Industrial Aerodynamics, 59, pp. 233-246.

[5] Satake N, Suda K, Arakawa T, Sasaki A, and Tamura Y (2003). Damping evaluation using full-scale data of buildings in Japan. Journal of Structural Engineering, 129(4), pp. 470-477.

[6] Sohn H, Farrar CR, Hemez FM, Shunk DD, Stinemates DW and Nadler BR (2003). A review of structural health monitoring literature: 1996-2001. Los Alamos National Laboratory Report, LA-13976-MS.

[7] Yuen KV and Katafygiotis LS (2003). Bayesian Fast Fourier Transform Approach for modal updating using ambient data. Advances in Structural Engineering, 6(2), pp. 81-95.